

On the nature of dust clouds in the region towards M 81 and NGC 3077

Andreas Heithausen

I. Physikalisches Institut, Universität Köln, Zùlpicher Str. 77, 50937 Köln, Germany, e-mail: aheithau@uni-koeln.de *

Received 9 Aug 2011; accepted 18 May 2012

ABSTRACT

Aims. There is some controversy on the nature of dust clouds found in direction of the interacting galaxy triplet M 81, M 82, and NGC 3077. Are they associated with the tidal arms seen in HI around those galaxies or are they simply Galactic foreground clouds?

Methods. Data from the SPIRE instrument onboard HERSCHEL** and MIPS onboard of SPITZER are used to derive physical parameters for the dust clouds. These observations are compared to CO clouds previously mapped with the IRAM and the FCRAO radio telescopes.

Results. SPIRE and MIPS maps show several dust clouds north of M 81 and south of NGC 3077. Modelling of the dust emission provides total hydrogen column densities between 1.5 and $5.0 \cdot 10^{20} \text{ cm}^{-2}$. Dust temperatures are between 13 to 17 K. No significant difference in the dust emission can be found between individual clouds. It is shown that CO line emission provides the best clues on the origin of those clouds. Most of the clouds seen towards M 81 are associated with small-area molecular structures (SAMS), i.e. tiny CO clouds of Galactic origin. The clouds seen towards NGC 3077 are partly associated with the tidal arms and are partly in the Galactic foreground associated with SAMS.

Key words. ISM: clouds – ISM: individual objects: SAMS1, SAMS2 – ISM: molecules – galaxies: individual: M 81, NGC 3077, Arp’s loop

1. Introduction

Interpretation of astronomical observations is always hampered by the lack of direct distance information. Whether or not objects on the same line-of-sight are indeed physically related is not easy to judge. Directly linked to this question is the problem of finding dust in the intergalactic medium (Xilouris et al. 2006; Walter et al. 2011). One well studied region where this problem becomes obvious is the region towards M 81, M 82, and NGC 3077. It is one of the closest sample of interacting galaxies. HI tidal arms are found to connect these three galaxies (Yun et al. 1994). Especially since the discovery of Arp’s loop (Arp 1965) there has been some debate about the nature of interstellar clouds in that region: are they related to tidal arms around the interacting galaxy triplet (Sun et al. 2005; de Mello et al. 2008) or to Galactic foreground cirrus (Sollima et al. 2010; Davies et al. 2010)?

Sandage (1976) presented deep optical images that showed that the M 81-M 82-NGC 3077 region is seen through wide spread Galactic foreground cirrus clouds. De Vries et al. (1987) presented large-scale maps with an angular resolution of 9 arcmin of atomic hydrogen, carbon monoxide and dust infrared emission, which showed Galactic cirrus emission towards the M 81 triple with total hydrogen column densities of about $1\text{--}2 \cdot 10^{20} \text{ cm}^{-2}$. In most cases it is possible to distinguish between an extragalactic or Galactic origin of the dust and gas because the radial velocities are very different from each other. In the case of

the M 81 region however the radial velocities of Galactic and extragalactic gas share (at least partly) the same LSR velocity range close to zero.

Significant substructure in the Galactic foreground gas was detected by Heithausen (2002) who found several small-area molecular structures (SAMS) towards the outer regions of M 81 and NGC 3077. SAMS are tiny molecular clouds detected in a region where the shielding of the interstellar radiation field is too low for them to survive for a long time (Heithausen 2002). The CO clouds are less than one arcmin wide, corresponding to linear sizes below 6000 AU at an adopted distance of 100pc. High angular resolution observations obtained with the Plateau de Bure interferometer show substructure down to the resolution limit of 3'' (approx. 300 AU) with indication of further unresolved structure (Heithausen 2004).

So far, one such cloud has been detected towards the tidal arms around NGC 3077 and four in the region around M 81 (Heithausen 2006). The agreement of the LSR velocities of SAMS with that of the Galactic HI gas shows that they are of Galactic origin. Furthermore their CO linewidths are too narrow for extragalactic objects. At an adopted distance of about 100pc their masses are about that of Jupiter.

The purpose of this paper is twofold: first independent estimates on column densities and temperatures of SAMSs are obtained, second these objects are used to distinguish between Galactic foreground clouds and extragalactic tidal arm clouds. The outline of the paper is as follows: after a brief description of the infrared data the resulting spectral energy distributions (SEDs) are used to determine dust column densities and temperatures and find new SAMS candidates; one of those could directly be confirmed as molecular cirrus cloud with existing CO data. Based on published CO data the dust clouds are classified

* New address: Institut für Physik und ihre Didaktik, Universität zu Köln, Gronewaldstr. 2, 50931 Köln, Germany

** *Herschel* is an ESA space observatory with science instruments provided by European-led Principal Investigator consortia and with important participation from NASA.

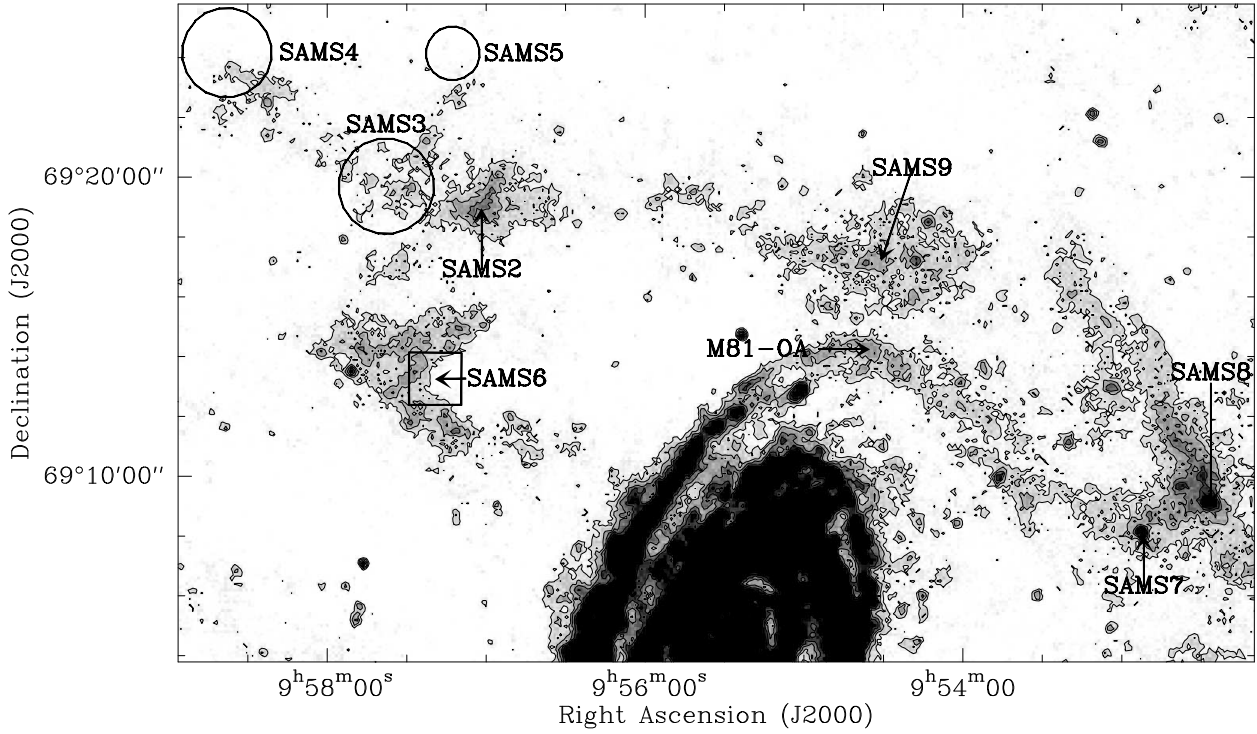


Fig. 1. SPIRE 250 μm map of the area surrounding SAMS2. Contours are from 0.02 to 0.1 Jy beam⁻¹ every 0.02 Jy beam⁻¹. The intense emission at the lower centre of the map originates from M 81. The positions of the sources discussed in this paper are labeled. The weak clouds SAMS 3-5 are marked by circles with the approximate size of the clouds. The square marks the area of SAMS6 over which spectra have been averaged to detect a weak CO line (s. Fig. 4).

as Galactic or extragalactic. It is shown that the dust clouds towards M 81 are most likely Galactic foreground clouds, whereas the clouds seen towards NGC 3077 are partly associated with the tidal arms and are partly in the Galactic foreground.

2. Observations

For the analysis in this paper I used photometric data obtained with the SPIRE (Griffin et al. 2010) onboard of the Herschel satellite and with MIPS (Rieke et al. 2004) onboard of the Spitzer satellite. Calibrated data of the M 81 region obtained with SPIRE were retrieved from the Herschel archive (level 2 products). A first analysis of the data is presented by Bendo et al. (2010) to study the dust content and temperature of the spiral galaxy. SPIRE data of NGC 3077 were obtained from the open time key project KINGFISH (Walter et al. 2011).

The SPIRE data are given in Jy beam⁻¹; to convert the data to MJy sr⁻¹ beam areas of 447, 816, and 1711 arcsec⁻¹ were assumed for the 250, 350, and 500 μm bands (Sibthorpe et al. 2011). The calibration uncertainties for the individual bands are 7% (SPIRE Observer's Manual 2011). At 250, 350 and 500 μm SPIRE has a slightly elliptical beam of 18.7'' \times 17.5'', 25.6'' \times 24.2'' and 38.2'' \times 34.6'', respectively (Sipthorpe et al., loc.cit.) for pixel scales of 6, 10, and 14 arcsec.

For the M 81 region photometric data at 70 and 160 μm obtained with Spitzer MIPS were retrieved from the SINGS archive (Kennicutt et al. 2003). Corresponding data at 160 μm for the region around NGC 3077 were taken directly from the Spitzer archive. For this region three data sets exist in the archive which cover the clouds of interest completely, though part of the more extensive diffuse emission around the galaxy might be missing. Because the signal-to-noise level of a single set is already high enough (larger than 10 for the weakest cloud) I only used one

data set (AOR 17597952), after checking that the data set is comparable with the other sets (AORs 17598208 and 17597696). The data sets are calibrated in MJy/sr. The FWHM of the point-spread function (PSF) is 18'', and 40'' at 70 μm and 160 μm , resp. (Engelbracht et al. 2004). The accuracy of the photometric calibration of the two bands was estimated to be 5% at 70 μm (Gordon et al. 2007) and 12% at 160 μm (Stansberry et al. 2007).

Additionally to the photometric observations, the IRAM 30 m telescope has been used to search for extensive ¹²CO (1 \rightarrow 0) emission around SAMS1 in June 2001. Observations were done with a wobbling subreflector with an off-position separated by 200'' in azimuth from the on-position. An autocorrelator spectrometer was used with a velocity resolution of 0.2 km s⁻¹. The angular resolution of the telescope at 115 GHz was 22''. The data were processed using the standard data reduction software for radioastronomical spectra GILDAS¹. Only linear baselines were removed from the spectra.

3. Results

3.1. The region towards M 81

The SPIRE 250 μm map of the M 81 region is presented in Fig. 1. Dust is concentrated in several small filaments. Six clouds are identified outside the main body of M 81. Positions of the local maxima are listed in Tab. 1.

For comparison the distribution of the total HI gas of this region taken from the THINGS project (Walter et al. 2008) is displayed in Fig. 2. The velocity range of the naturally weighted maps covers about 250 km s⁻¹. Note that because the interferometer data are not corrected for missing zero spacing exten-

¹ see <http://www.iram.fr/IRAMFR/GILDAS/>

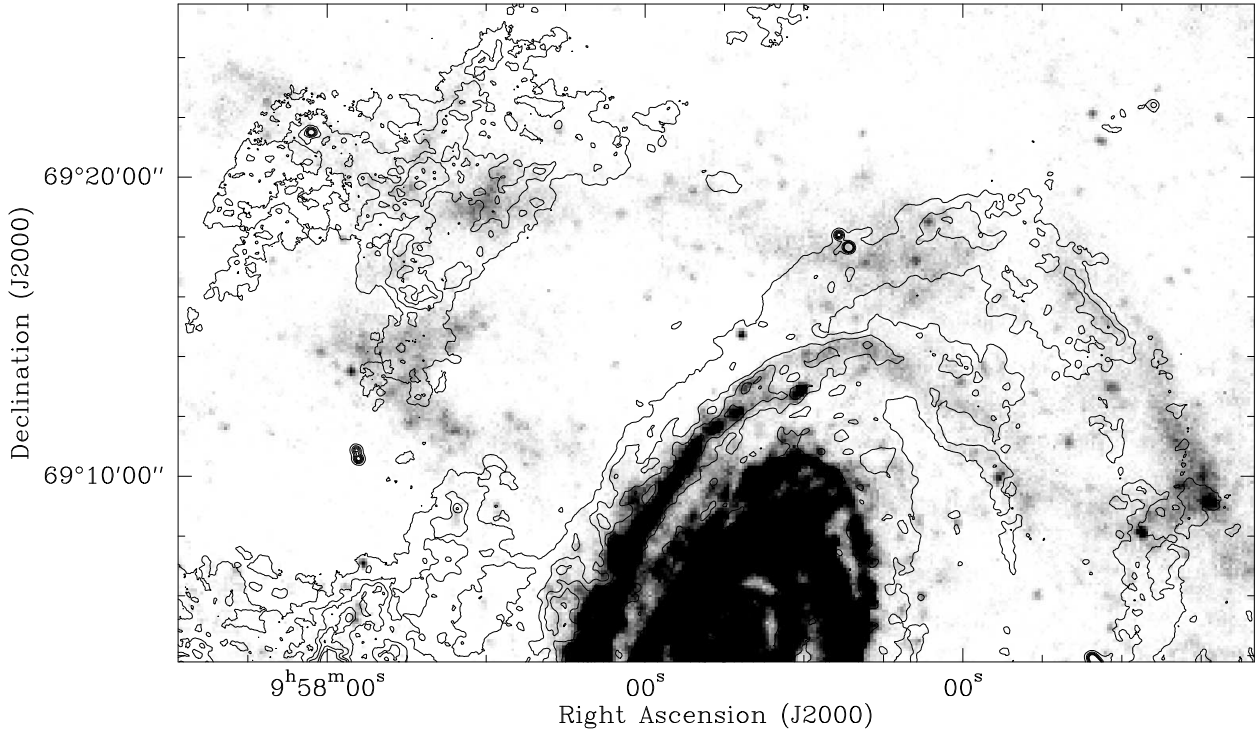


Fig. 2. THINGS total HI map (contours, Walter et al. 2008) of the area surrounding M 81 overlaid on the SPIRE 250 μm map (greyscale). The map has been integrated over a velocity range of about 250 km s^{-1} . Contours are from 50 to 500 $\text{Jy beam}^{-1} \text{m s}^{-1}$ every 100 $\text{Jy beam}^{-1} \text{m s}^{-1}$.

sive HI emission has been filtered out. Due to the small size of the dust clouds this is however not critical for the analysis. The distribution of HI associated with the spiral arms of M 81 shows a close similarity to the dust. The HI clouds associated with the tidal arms of M 81 show however no obvious morphological similarity to the dust clouds. Davies et al. (2010) already noted that a much greater similarity can be found when comparing the infrared data with a single velocity channel of the HI data at velocities close to zero, i.e. that which correspond to Galactic velocities.

A morphological similarity can be found when one compares the dust with the CO emission from small-area molecular structures, too. SAMS2 (Heithausen 2002) can clearly be identified in all SPIRE bands (compare Figs. 1 and 3) and in the MIPS 160 μm band. The other molecular structures in its vicinity found in CO observations with the FCRAO 14m telescope (Heithausen 2006) are detected in the 250 μm map, too. Note that the CO data have a coarser angular resolution of only 45'' compared to the SPIRE 250 μm data and are very weak ($T_A^* < 0.1 \text{ K}$).

There is one further dust cloud in the FCRAO field (compare Fig. 1 and 3) previously undetected in CO (labelled SAMS6 in Fig. 1). To see whether molecular gas is associated with that cloud the spectra obtained with the FCRAO 14m telescope (Heithausen 2006) were averaged over areas of 60'' by 60''. In those spectra four neighboring positions with marginal CO detections can be found centered on the Galactic coordinates $(l, b) = (141^\circ.802, 40^\circ.936)$ which corresponds to $(\alpha, \delta) = (09^{\text{h}}57^{\text{m}}18^{\text{s}}.5, +69^\circ13'22''.4)$. The average of those positions is shown in Fig. 4. Here a clear CO line has been detected with the following values obtained from a Gaussian fit to the data: amplitude $T_A^* = 0.032 \pm 0.008 \text{ K}$, center velocity $v_{\text{LSR}} = 3.6 \pm 0.1 \text{ km s}^{-1}$, and line width $\Delta v = 1.8 \pm 0.3 \text{ km s}^{-1}$. These values are similar to those of previous detected SAMS.

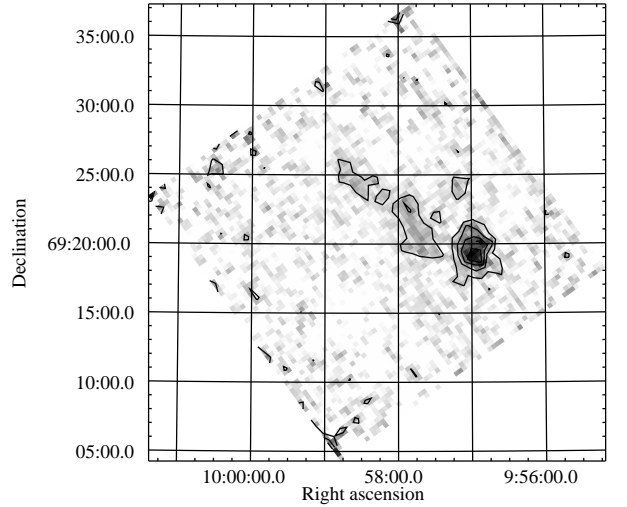


Fig. 3. Integrated CO map obtained with the FCRAO 14 m radiotelescope (Heithausen 2006). Contours are every 0.04 K km s^{-1} starting at 0.04 K km s^{-1} .

For the further quantitative analysis (Sec. 3.3) six apparent cirrus clouds are identified, three of which show CO emission of clear Galactic origin (SAMS2, 4, and 6) while for the other three such observations are not yet available (labelled SAMS7, 8, and 9 in Tab. 1 and Fig. 1). Although SAMS3 and SAMS5 show CO emission, they are not considered further because they are hard to identify in the SPIRE 350 and 500 μm bands. For comparison

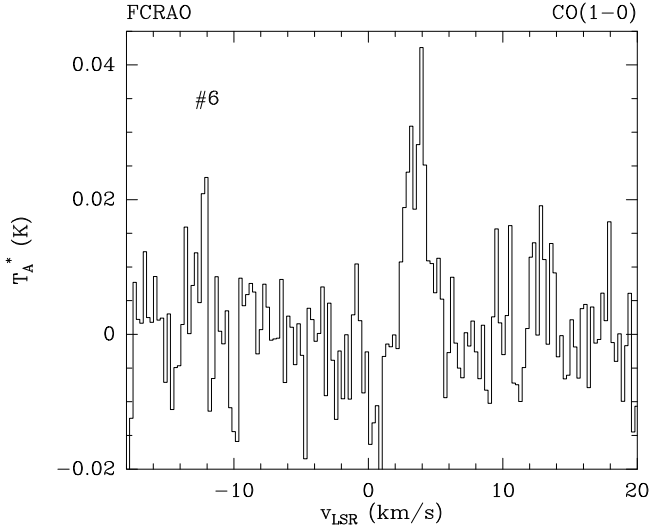


Fig. 4. CO 1 → 0 spectrum of the newly detected SAMS6 centered on $(\alpha, \delta) = (09^h57^m18^s.5, +69^\circ13'22''.4)$

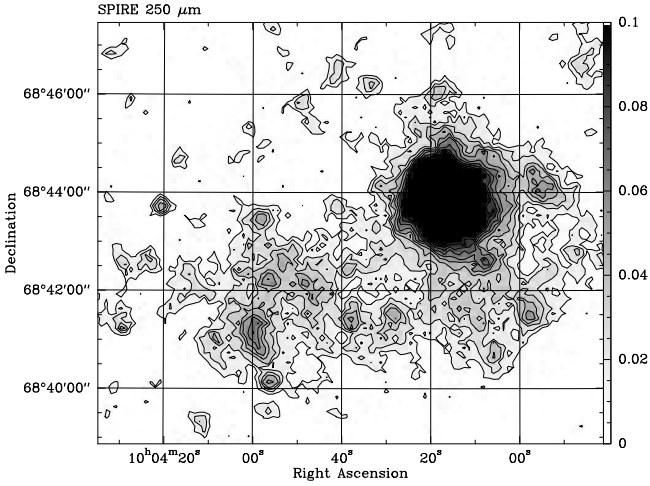


Fig. 5. Spire 250 μm map of the region towards NGC 3077 as observed by Walter et al. (2011). Contours are from 0.01 to 0.08 Jy beam $^{-1}$ every 0.01 Jy beam $^{-1}$. The intense emission in the right half of the map originates from NGC 3077.

one cloud in an outer spiral arm of M 81 (labelled M 81-OA is also listed in Tab. 1).

3.2. The region towards NGC 3077

NGC 3077 is the smallest member of the interacting M 81 galaxy triple. Intense HI tidal arms have been found surrounding this galaxy (Yun et al. 1994). Towards these arms Walter & Heithausen (1999) have detected a giant molecular complex. Walter et al. (2011) have used the SPIRE instrument to search for the thermal emission of dust associated with the tidal arms. A map at a wavelength of 250 μm is presented in Fig. 5. Based on a positional coincidence Walter et al. attribute all of the emission they found in that region to the tidal arms around NGC 3077. In this section it is shown that at least some part is most likely associated with Galactic foreground clouds.

In the region towards NGC 3077 we are faced with two molecular clouds, one of clear extragalactic and one of clear Galactic origin. The situation is displayed in Fig. 6. The distinc-

tion can be made based on the CO linewidth and LSR velocity. The extragalactic cloud complex (Walter & Heithausen 1999, Heithausen & Walter 2000) shows CO linewidths of several km s $^{-1}$ and velocities slightly outside that of the local Galactic gas (solid contours). Next to this complex is the small-area molecular structure SAMS1 (dashed contours, Heithausen 2002) with a linewidth of below 1 km s $^{-1}$ and LSR velocities in agreement with that of local Galactic HI gas.

Beyond the CO map of SAMS1 presented in Fig. 6 further CO (1 → 0) emission has been detected with the IRAM 30m telescope towards the position $(\alpha, \delta) = (10^h03^m08^s.4, +68^\circ40'31''.8)$. A Gaussian fit to the data gives a amplitude $T_A^* = 0.055 \pm 0.004$ K, a center velocity $v_{\text{LSR}} = 3.47 \pm 0.14$ km s $^{-1}$, and a line width $\Delta v = 1.6 \pm 0.3$ km s $^{-1}$. (The LSR velocity corresponds to a heliocentric velocities of $v_{\text{Hel}} = -2.53$ km s $^{-1}$.) These values are similar to that of SAMS1, i.e. the molecular gas is of Galactic origin.

Both the Galactic and the extragalactic clouds are associated with emission in the 250 μm band (s. Fig. 6) as well as with emission in the 350 and 500 μm band. For further quantitative analysis three extragalactic regions (NGC 3077-TA1 to TA3) and one Galactic cloud (SAMS1) are identified (see Tab. 1). These positions are associated with the most intense regions in this SPIRE 250 μm map outside the main body of NGC 3077.

3.3. SEDs

To obtain dust column densities and temperatures the IR maps were smoothed to the same angular resolution and intensities averaged over square areas with 40'' width were obtained. Background correction were obtained in fields close to the observed regions which show no obvious emission. Derived intensities for the individual spectral bands are listed in Tab. 1. The uncertainties for the values are estimated from the noise level (1σ) in regions, which are apparently free of emission. For the M 81 region these values are found to be at 0.60, 0.38 and 0.21 MJy sr $^{-1}$ for the Herschel 250, 350, and 500 μm bands and 0.5 MJy sr $^{-1}$ for both the MIPS 70 and the 160 μm bands. For the NGC 3077 region the corresponding values are 0.55, 0.27 and 0.16 MJy sr $^{-1}$ for the Herschel 250, 350, and 500 μm bands and 0.5 MJy sr $^{-1}$ for the MIPS 160 μm band, respectively.

A blackbody fit is used to derive dust temperatures and hydrogen column densities of the observed regions. Assuming optically thin emission the observed intensity I_ν can be modelled as

$$I_\nu = B_\nu \cdot m_H \cdot \mu \cdot N_H \cdot \kappa_\nu$$

where B_ν is the Planck function and N_H is the total hydrogen column density (cf. Ward-Thompson et al. 2010). $m_H \cdot \mu$ is the mean mass of a particle in the cloud with m_H being the mass of an hydrogen atom; μ was adopted to be 2.3 (cf. Ade et al. 2011). Following Beckwith et al. (1990) the dust mass opacity κ_ν is parameterized as

$$\kappa_\nu = 0.1 \text{ cm}^2 \text{ g}^{-1} \cdot \left(\frac{\nu}{1000 \text{ GHz}} \right)^\beta$$

For the fit a dust opacity index $\beta = 2$ has been adopted, which is consistent with the value used by André et al. (1993) for molecular cores. Fits to the data are displayed in Fig. 7; derived temperatures and total hydrogen column densities are listed in Tab. 1.

The derived dust temperatures are within the range of 13 to 17 K with an uncertainty of $\Delta T = \pm 2$ K for individual values. There is no significant difference between the dust temperature of the outer arm of M 81, the tidal arm features close

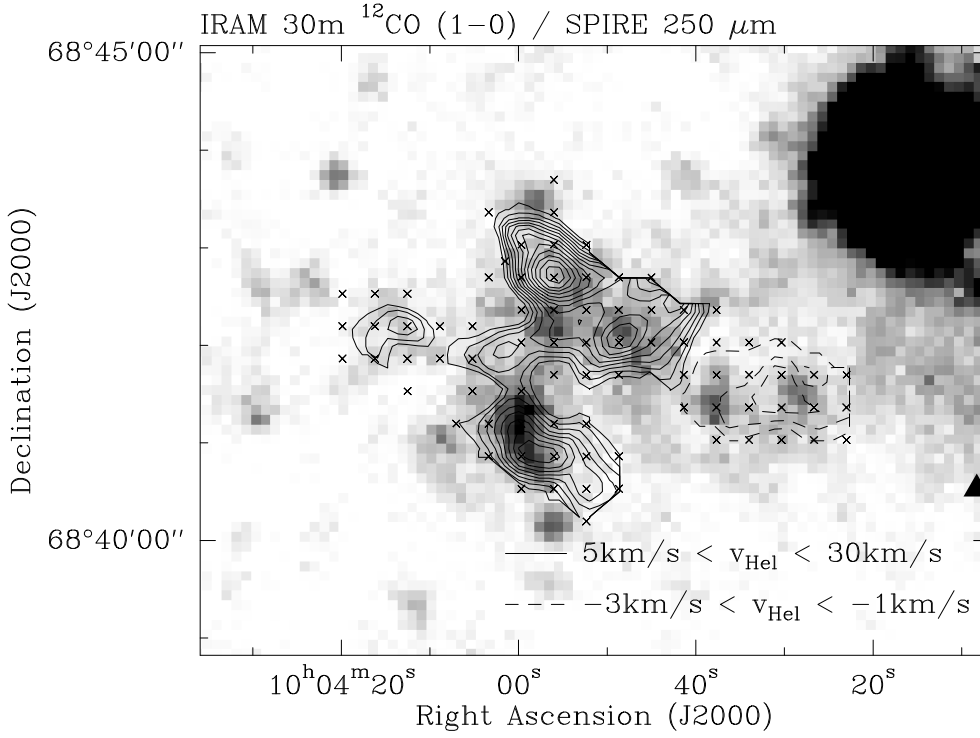


Fig. 6. Spire 250 μm map of the region towards NGC 3077 overlaid with contours from observations of the CO (1 \rightarrow 0) line obtained with the IRAM 30 m telescope (Heithausen 2002; Walter & Heithausen 1999; Heithausen & Walter (2000)). Observed CO positions are marked by Xs. Contours are from 0.1 K km s⁻¹ every 0.1 K km s⁻¹. Solid contours show emission from the tidal arm cloud associated with NGC 3077 (Walter & Heithausen 1999; Heithausen & Walter 2000), whereas dashed contours show emission from the Galactic small area molecular structure SAMS1 (Heithausen 2002). There is further CO emission towards the position (α, δ) = (10^h03^m08^s.4, +68°40'31''.8), which is marked by the black triangle.

Table 1. Parameters of the dust clouds derived from SPIRE and MIPS data

Source	RA J2000	Dec J2000	$I_{250\mu\text{m}}$ MJy sr ⁻¹ SPIRE	$I_{350\mu\text{m}}$ MJy sr ⁻¹ SPIRE	$I_{500\mu\text{m}}$ MJy sr ⁻¹ SPIRE	$I_{70\mu\text{m}}$ MJy sr ⁻¹ MIPS	$I_{160\mu\text{m}}$ MJy sr ⁻¹ MIPS	T_{Dust} K	N_{H} 10 ²⁰ cm ⁻²
SAMS1	10:03:28.4	68:41:29.2	3.9	2.1	1.0	...	4.5	14.5	1.8
NGC 3077-TA1	10:04:00.6	68:41:09.9	5.7	3.6	2.0	...	4.9	13	5.4
NGC 3077-TA2	10:03:55.4	68:42:39.4	4.2	2.7	1.5	...	5.1	13	3.5
NGC 3077-TA3	10:03:48.0	68:42:01.4	4.7	2.8	1.6	...	5.1	13	3.6
SAMS2	9:57:01.0	69:19:05.4	7.6	3.5	1.5	≤ 0.5	7.4	16	3.3
SAMS3	9:57:36.8	69:19:48.7	3.6
SAMS4	9:58:36.5	69:24:16.8	4.6	2.3	0.9	13.5	3.7
SAMS5	9:57:11.9	69:24:15.3	2.7
SAMS6	9:57:18.5	69:13:22.4	5.7	3.0	1.5	≤ 0.5	6.7	15.5	3.1
SAMS7	9:52:53.1	69:08:09.6	8.6	3.8	1.5	2.9 ¹	8.0	16.5	3.1
SAMS8	9:52:28.0	69:09:06.8	11.2	5.2	1.9	≤ 0.5	10.9	14.5	7.2
SAMS9	9:54:31.4	69:17:19.5	6.3	3.4	1.6	≤ 0.5	5.4	13	6.9
M 81-OA	9:54:35.5	69:14:22.0	6.5	3.6	1.3	≤ 0.5	5.5	14	5.1

Notes. 1: possible contributions from a point source

to NGC 3077, and the Galactic foreground clouds. The values are similar to those derived for typical cirrus clouds as e.g. the Polaris Flare where the average dust temperature was found to be $T_D = 14.5 \pm 1.6$ K (Miville-Deschênes et al. 2010). These values agree also well with those estimated from excitation conditions of the CO line between 7 to 20 K (Heithausen 2004), although gas and dust are not necessarily coupled.

The total hydrogen column densities estimated from the SED fit are within 1.8 and $7.2 \cdot 10^{20} \text{ cm}^{-2}$. The uncertainty is estimated to be $\pm 0.5 \cdot 10^{20} \text{ cm}^{-2}$. Again no significant difference between extragalactic and Galactic clouds is apparent. For SAMS1 Heithausen (2002) found an HI column density of $N(\text{HI}) = 1.3 \cdot 10^{20} \text{ cm}^{-2}$ and an H₂ column densities of $N(\text{H}_2) = 0.7 \cdot 10^{19} \text{ cm}^{-2}$ and for SAMS2 $N(\text{HI}) = 2.1 \cdot 10^{20} \text{ cm}^{-2}$ and $N(\text{H}_2) = 3.7 \cdot 10^{19} \text{ cm}^{-2}$. The sums of $N(\text{H}) = N(\text{HI}) + 2 \cdot N(\text{H}_2)$ agree well with the values derived here from the IR emission for both clouds.

4. Discussion

4.1. SAMS

Previous estimates on the kinetic temperatures and masses of SAMSS (Heithausen 2002, 2006) were made using HI and CO data assuming that the physical parameters are similar to those of Galactic cirrus clouds. While the determination of the atomic hydrogen column density is straightforward from its 21cm line, the determination of the molecular hydrogen column density is more difficult. It is based on an empirically determined conversion factor X_{CO} applied to the velocity integrated CO line. For SAMS the low value found for the large scale foreground clouds (de Vries et al. 1987) had been used.

SPIRE and MIPS data now provide an independent means to estimate the dust temperatures and masses of SAMSS. In this paper the values were derived adopting a gas-to-dust mass ratio of 100, which is well within the values found for our Galaxy

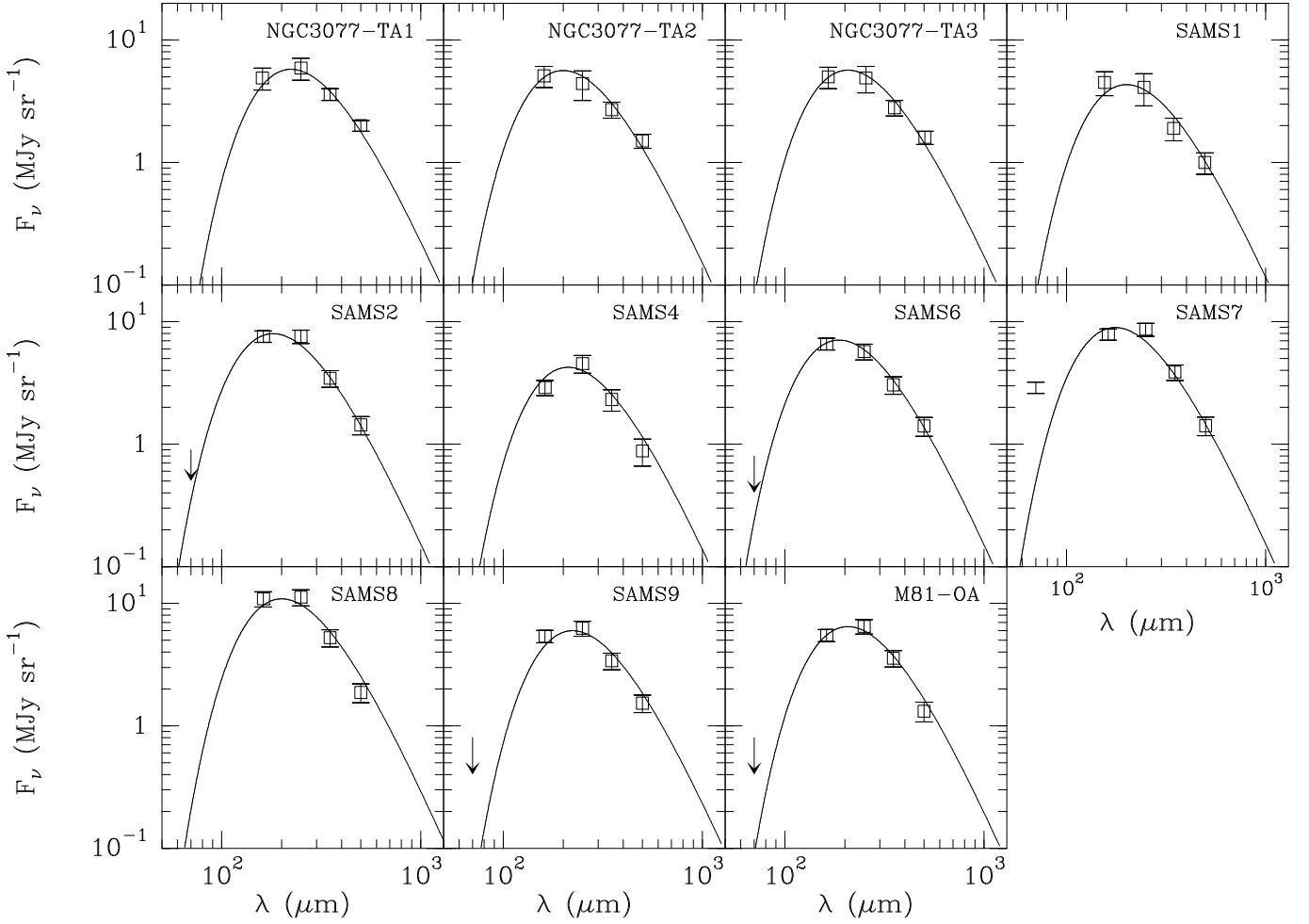


Fig. 7. Dust spectra of the observed sources obtained from the SPIRE and MIPS bands. Each point gives the mean intensity of a field covering an area of $40'' \times 40''$. Solid lines are fits to the data. For the fits $\beta = 2$ has been adopted. The $160\mu\text{m}$ intensity of SAMS7 shows contributions from a point source.

(Sodroski et al. 1997). These new estimates confirm the previous ones, namely that SAMSs have low total hydrogen column densities and, following from that, low masses, comparable to that of Jupiter. Their temperatures are between 13 and 17 K. SAMSs therefore form most likely the very low mass end of molecular clouds in the Galactic cirrus. As such they can provide valuable clues for the understanding of the formation or destruction of molecular clouds in our Galaxy.

Note that this set of observations however does not provide independent clues on the metallicity of the clouds for the following reason: the X_{CO} factor is found to increase with decreasing metallicity (e.g. Wilson 1995, Barone et al. 2000). For a given CO intensity a lower metallicity would therefore result in a higher H_2 column density. Similarly, the gas-to-dust ratio increases with decreasing metallicity. For a lower metallicity a given infrared intensity would thus result in a higher H_2 column density, too.

4.2. Tidal arms or Galactic cirrus clouds?

The dust temperatures and column densities of the clouds examined in this paper are very similar. Based on the assumption of a Galactic dust-to-gas ratio total hydrogen column densities are found to be in the range between 1.8 and $7.2 \cdot 10^{20} \text{ cm}^{-2}$. Dust temperatures are between 13 to 17 K. There is no obvious

difference between the individual clouds. So there is no way to distinguish between Galactic and extragalactic origin based on dust color ratios or infrared intensity alone.

In the region towards M 81 at least three out of six clouds are clearly detected in CO lines of Galactic origin. The other filamentary clouds have similar structures and similar intensities in the SPIRE bands. They are thus candidates for small-area molecular structures which have however to be verified by deep CO observations.

Comparison of deep optical images (e.g. given in Sollima et al. 2010) with the SPIRE $250\mu\text{m}$ map shows that the clouds detected in CO (SAMS2, 4, and 6) are morphological very similar. These dust clouds form part of the structure known as Arp's ring or loop (Arp 1965). The narrow CO linewidth and the close agreement of the line of sight velocities with local HI gas (Heithausen 2002, 2004) clearly rule out an extragalactic origin of this structure. We are thus just faced with a chance superposition of foreground filaments forming a loop like structure with the distant galaxy M 81. The observations presented in this paper thus confirm the conclusions of Sollima et al. (2010) who, based on HI and dust observations, found that the bulk of dust emission outside the main body of M 81 is associated with Galactic cirrus clouds. Davies et al. (2010) describe a break-down of the HI-infrared relation on scales below 1 arcmin. This could be caused

by the fact that the clouds become at least partly molecular, as can be seen by the detection of CO towards some of these clouds.

Towards NGC 3077 the situation is more complex: here we are faced with one molecular cloud of Galactic and another molecular complex of extragalactic origin. Both show up in all SPIRE bands with similar color ratios. Our incomplete CO map presented in this paper shows that the Galactic cloud SAMS1 is probably more extended than previously thought. This suggests that even more of the dust seen towards NGC 3077 is located in the Galactic foreground. Walter et al. (2011) attributed all SPIRE emission to the tidal tail of NGC 3077, whereas it is shown here that some of the IR emission is of Galactic origin.

5. Conclusions

The data presented in this paper show that the mere coincidence of HI gas and dust emission on the same line of sight does not prove that the clouds are really physically associated, even if the intensity maxima partly coincide. CO gas is a much better indicator for an association. The velocity information of the CO spectral lines provides valuable clues on the origin of the gas and the associated dust, either Galactic or extragalactic. To confirm or exclude either origin, CO spectra should therefore cover a bandwidth which includes both Galactic and extragalactic velocities. Because in some cases such a configuration is not possible with the receiver, the observer should consider to take at least some control spectra covering Galactic velocities.

Clearly, more extensive CO observations of the Galactic cirrus clouds are demanded to study the importance of small area molecular structures. Currently most of such surveys for molecular cirrus clouds are done with moderate to low angular resolution (Heithausen et al. 1993; Magnani et al. 2000; Onishi et al. 2001). Due to the small size of SAMSSs these observations should be conducted at high angular resolution and high sensitivity. As shown in this paper emission at 250 to 500 μm could be a good guide to find such clouds.

Finally, it would be interesting to study if there are more examples of dust clouds where their origin, either Galactic or extragalactic, is not clear. Two such cases have been reported by Dirsch et al. (2003; 2005) and by Cortese et al. (2010). Dirsch et al. found a single dense cloud of only 4'' diameter projected on a spiral arm of the galaxy NGC 3269. Based on a study of the reddening law of that object the authors conclude that it has a Galactic origin. Cortese et al. describe a system of interacting galaxies similar to that of M 81. Towards NGC 4435/4438 they found a HI, CO, and dust cloud which could be interpreted as tidal stream or as Galactic foreground cirrus. Based on velocity information of HI and CO spectra the authors favour a Galactic origin. The width of their CO line of only $\Delta v = 1.5 \text{ km s}^{-1}$ is similar to that of SAMSS (Heithausen 2006), i.e. more consistent with Galactic cirrus clouds than with extragalactic molecular complexes. It is certainly worthwhile to map the total extent of the molecular cloud in the NGC 4435/4438 field and to search CO towards NGC 3269, because they could be similar to the SAMSSs described in this paper.

Acknowledgements. I thank Fabian Walter for critical comments on the manuscript.

SPIRE has been developed by a consortium of institutes led by Cardiff University (UK) and including Univ. Lethbridge (Canada); NAOC (China); CEA, LAM (France); IFSI, Univ. Padua (Italy); IAC (Spain); Stockholm Observatory (Sweden); Imperial College London, RAL, UCL-MSSL, UKATC, Univ. Sussex (UK); and Caltech, JPL, NHSC, Univ. Colorado (USA). This development has been supported by national funding agencies: CSA (Canada); NAOC (China); CEA, CNRS (France); ASI (Italy); MCINN (Spain); SNSB (Sweden); STFC (UK); and NASA (USA).

References

- Ade, P.A.R., Aghanim, N., Arnaud, M. et al., 2011, *A&A*, 536, A22
 André, P. Ward-Thompson, D., Barsony, M., 1993, *ApJ*, 406, 122
 Arp, H., 1965, *Sci*, 148, 363
 Barone, L.T., Heithausen, A. Hüttemeister, Fritz, T., Klein, U., 2000, *MNRAS*, 317, 649
 Beckwith, S., Sargent, A.I., Chini, R., Güsten, R., 1990, *AJ*, 99, 924
 Bendo, G.J., Wilson C.D., Pohlen, M., et al., 2010, *A&A*, 518, L65
 Cortese, L., Bendo, G.J., Isaak, K.G., Davies, J.I., Kent, B.R., 2010, *MNRAS*, 403, L26
 Dirsch, B., Richtler, T., Bassino, L., 2003, *A&A*, 408, 929
 Dirsch, B., Richtler, T., Gomez, M., 2005, *AJ*, 130, 1141
 Davies, J.I., Wilson, C.D., Auld, R., et al., 2010, *MNRAS*, 409, 102
 de Mello, D.F., Smith, L.J., Sabbi, E., Gallagher, J.S., Mountain, M., Harbeck, D.R., 2008, *AJ*, 135, 548
 de Vries, H.W., Heithausen, A., Thaddeus, P., 1987, *ApJ*, 319, 723
 Engelbracht, C.W., Gordon, K.D., Bendo, G.J. et al., 2004, *ApJS*, 154, 248
 Gordon, K.D. Engelbracht, C.W., Fadda, D. et al., 2007, *PASP*, 119, 1019
 Griffin, M.J., Abergel, A., Abreu, A., et al., 2010, *A&A*, 518, L3
 Heithausen, A., Stacy, J. G., de Vries, H. W., Mebold, U., Thaddeus, P. 1993, *A&A*, 268, 265
 Heithausen, A., Walter, F., 2000, *A&A*, 361, 500
 Heithausen, A., 2002, *A&A*, 393, L41
 Heithausen, A., 2004, *ApJ*, 606, L13
 Heithausen, A., 2006, *A&A*, 450, 193
 Kennicutt, R.C., Armus, L. Bendo, G. et al. 2003, *PASP*, 115, 928 (SINGS)
 Magnani, L., Hartmann, D., Holcomb, S.L., Smith, L.E., Thaddeus, P. 2000, *ApJ*, 535, 167
 Miville-Deschênes, M.A., Martin, P.G., Abergel, A., et al., 2010, *A&A*, 518, L104
 Onishi, T., Yoshikawa, N., Yamamoto, H., Kawamura, A. Mizuno, A., Fukui, Y., 2001, *PASJ*, 53, 1017
 Rieke, G.H., E. T. Young, E.T., Engelbracht C.W., et al., 2004, *ApJS*, 154, 25
 Sandage, A., 1976, *AJ*, 81, 954
 Sollima, A., Gil de Paz, A., Martinez-Delgado, D., Gabany, R.J., Gallego-Laborda, J.J., Hallas, T., 2010, *A&A*, 516, A83
 Sun, W.H., Zhou, X., Chen, W.P., Burstein, D., Windhorst, R.A., Ma, J., Byun, Y.L., Jiang, Z.J., Chen, J.S., 2005, *ApJ*, 630, L133
 Siphthorpe, B., Ferlet, M., Bendo, G. et al., 2011, http://ftp.sciops.esa.int/pub/hsc-calibration/SPIRE/PHOT/Beams/beam_release_note_v
 Sodroski, T.J., Odegard, N., Arendt, R.G., et al., 1997, *ApJ*, 480, 173
 SPIRE Observer's Manual, 2011, http://herschel.esac.esa.int/Docs/SPIRE/html/spire_om.html
 Stansberry, J.A., Gordon, K.D., Bhattacharya, B., et al., 2007, *PASP*, 119, 1038
 Walter, F., Heithausen, A., 1999, *ApJ*, 519, L69
 Walter, F., Brinks, E., de Blok, W.J.G., Bigiel, F., Kennicutt, R.C., Thornley, M.D., Leroy, A., 2008, *AJ*, 136, 2563
 Walter, F., Sandstrom, K., Aniano, G., et al., 2011, *ApJ*, 726, L11
 Ward-Thompson, D., Kirk, J.M., André, P. et al., 2010, *A&A*, 518, L92
 Wilson C. D., 1995, *ApJ*, 448, L97
 Xilouris, E., Alton, P., Alikakos, J., Xilouris, K., Boumis, P., Goudis, C., 2006, *ApJ*, 651, L107
 Yun, M.S., Ho, P.T.P., Lo, K.Y., 1994, *Nature*, 372, 530

List of Objects

- ‘M 81’ on page 1
- ‘NGC 3077’ on page 1
- ‘SAMS2’ on page 3
- ‘SAMS1’ on page 4